Water Science & Technology

IWA PUBLISHING

Water Science & Technology Vol 84 No 9, 2304 doi: 10.2166/wst.2021.449

A new insight into the restriction of Cr(VI) removal performance of activated carbon under neutral pH condition

Yi Fang [a,b], Ke Yang [a], Yipeng Zhang[a], Changsheng Peng[b,c], Aurora Robledo-Cabrera[a] and Alejandro López-Valdivieso[a,*]

[a] Instituto de metalurgia, Universidad Autónoma de San Luis Potosí, Av. Sierra Leona 550 C.P. 78210, San Luis Potosí, Mexico
[b] Guangdong Provincial Key Laboratory of Environmental Health and Land Resource, Zhaoqing University, Zhaoqing 526061, China
[c] The Key Lab of Marine Environmental Science and Ecology, Ministry of Education, Ocean University of China, Qingdao 266100, China
*Corresponding author. E-mail: alopez@uaslp.mx

YF, 0000-0003-4027-0323; KY, 0000-0002-8676-3097

ABSTRACT

Activated carbon has been widely used to remove hazardous Cr(VI); however, the impact of Cr_2O_3 precipitate on gradually declining removal ability as pH increases has received little attention. Herein, to investigate the effect of Cr_2O_3, SEM-EDX (scanning electron microscope-energy dispersive X-ray analysis) coupling elements mapping of chromium-loaded powdered activated carbon (PAC) revealed that a chromium layer was formed on the PAC exterior after being treated with Cr(VI) at pH 7. XPS (X-ray photoelectron spectroscopy) study confirmed that 69.93% and 39.91% Cr_2O_3 precipitated on the PAC surface at pH 7 and pH 3, respectively, corresponding to 17.77 mg/g and 20 mg/g removal capacity. Exhausted PAC had a removal efficiency of 92.43% after Cr_2O_3 being washed by H_2SO_4 solution, which was much higher than the removal efficiency of 51.27 % after NaOH washing. This further verified that the intrinsically developed Cr_2O_3 precipitate on PAC under neutral conditions limited the durability of PAC as an adsorbent. Consecutive elution assessments confirmed that adsorption and reduction ability both declined as pH increased. Raman spectroscopy and C 1s spectra of materials demonstrated two distinct Cr(VI) removal mechanisms under pH 3 and pH 7. In conclusion, the exhausted AC after Cr(VI) adsorption can be rejuvenated after the surface coated Cr_2O_3 is washed by the acid solution, which can expand the longevity of AC and recover Cr(III).

Key words: activated carbon, adsorption, chromium, neutral conditions, passivation, reduction

HIGHLIGHT

- In this work, we scrutinized the mechanism of poor removal capacity of commercial activated carbon on toxic heavy metal Cr(VI) under neutral pH conditions. Differing from the most accepted view that electrostatic repulsion is the main consideration, our study suggested that the relatively more Cr_2O_3 precipitate on the surface of activated carbon under higher pH led to the low Cr(VI) sequestration capability.

GRAPHICAL ABSTRACT

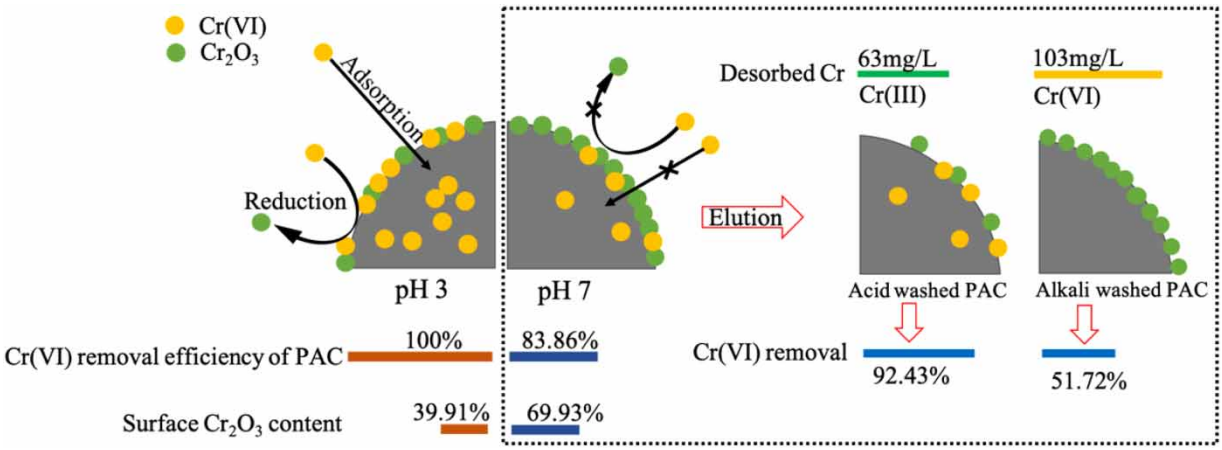

1. INTRODUCTION

Chromium abounds in nature and is highly toxic in the form of CrO_4^{2-} and $Cr_2O_7^{2-}$ through bioaccumulation (Li *et al.* 2018). The chromium pollution of water, land, and environment has attracted the interest of experts as electroplating plants, stainless steel manufacturing plants, leather manufacturing plants, and refractory plants have progressively appeared (Wang *et al.* 2019; Aparicio *et al.* 2021; Samuel *et al.* 2021). Cr(III) presents less mobility, toxicity, and solubility than Cr(VI) and generates sparingly soluble chromium hydroxides (Dognani *et al.* 2019). The reduction of Cr(VI) to Cr(III) is rapid at acidic conditions; meanwhile, the readily available electron is required for the reduction process (Deng *et al.* 2020; Fang *et al.* 2021b). It is well known that removing Cr(VI) from water by reduction and precipitation is a viable option (Barrera-Diaz *et al.* 2012; Qian *et al.* 2019; Wu *et al.* 2019; Zeng *et al.* 2019). Conventional reducing agents are sulfur and iron salts (Zhang *et al.* 2021a, 2021b); post-treated effluent that contained sulfate and iron salts would contaminate water and soil. Furthermore, the mandatory wastewater discharge would result in high costs.

The bulk of published studies on Cr(VI) removal by low-cost and readily accessible activated carbon (AC) demonstrated that removal capacity was greater in acidic conditions than alkaline conditions. This suggests that the Cr(VI) elimination is strongly pH dependent (Al-Othman *et al.* 2012; Zhou *et al.* 2016; Valentín-Reyes *et al.* 2019). The removal efficiency of Cr(VI) by activated carbon prepared from teakwood sawdust was 100% at pH 2, while it was below 20% at pH 10 (Ramirez *et al.* 2020). Table 1 shows the capacity of several ACs to remove Cr(VI) in acidic and alkaline environments. At low pH, the removal capacity was favored because the positively charged surface of Cr(VI) advanced the adsorption of anion Cr(VI) (Norouzi *et al.* 2018). It is worth noting that the pH-speciation of Cr(VI) reveals that $HCrO_4^-$ dominated below pH 6, whereas CrO_4^{2-} dominates above pH 7 (Rakhunde *et al.* 2012). Furthermore, prior studies have found that positively charged AC produced by protonation at a low pH value tends to attract chromate anions, which is thought to be the main mechanism for Cr(VI) adsorption (Mohan *et al.* 2005). It was discovered that as pH dropped, the reduction and adsorption process enhanced simultaneously.

To our understanding, there have been few investigations on systematic chromium adsorption and reduction study when pH rises over 7, to shed light on a substantial drop in AC performance. Most studies have only focused on the unfavorable effect of electrostatic repulsion between chromate anions and negatively charged AC surface at high pH values (Niazi *et al.* 2018; Ma *et al.* 2019; Liu *et al.* 2020). Besides, an earlier study failed to elucidate the removal paths at pH higher than 6 because the surface negatively charged bamboo bark-based AC that unfavored the adsorption of Cr(VI) anions, hence the reduction process of Cr(VI) to Cr(III) at high pH was omitted (Zhang *et al.* 2015). Cr(III) speciation as a function of pH was depicted clearly by Lopez-Valdivieso's study showing that $Cr(OH)_3(s)$ predominates at pH over 6.4 (Fang *et al.* 2021a). The effect on the removal of Cr(VI) under alkaline conditions of the AC surface loaded Cr(III) precipitate was especially neglected. Early reported studies on the synthesis of eskolaite (α-Cr_2O_3) nanoparticles through AC following adsorption of Cr(VI) have shown that Cr_2O_3 was the reduced species of Cr(VI) on AC (Cruz-Espinoza *et al.* 2012; Ibarra-Galván *et al.* 2014). Recently study showed that the Cr_2O_3 reduced the adsorption rate of Cr(VI) significantly (Wang *et al.* 2020).

Table 1 | Comparison of Cr(VI) removal under different pH by various carbon materials

Carbon materials	Cr(VI) removal capacity (mg/g)		References
	Acid condition	Alkali condition	
AC derived from *Posidonia Oceanica* seagrass	30.5 (pH 3)	0 (pH > 4)	Asimakopoulos *et al.* (2021)
Biochar derived from corn straw	125 (pH 2)	50 (pH 6)	Qu *et al.* (2021)
Powdered AC	46 (pH 2)	8 (pH 7)	Sangkarak *et al.* (2020)
Biochar derived from waste glue residue	206.7 (pH 2)	90 (pH 6)	Shi *et al.* (2020)
AC prepared by calcination of wheat bran	22 (pH 2)	0 (pH 10)	Ogata *et al.* (2020)
Commercial AC	21 (pH 2.5)	13 (pH 5.5)	Wu *et al.* (2020)
KOH activated porous corn straw	98.3 (pH 3)	33.7 (pH 7)	Ma *et al.* (2019)
AC derived from an acrylonitrile-divinylbenzene copolymer	80 (pH 2)	9 (pH 8)	Duranoğlu *et al.* (2012)

Compared to the consensus that the electrostatic repulsion led to poor Cr(VI) removal efficiency of AC in alkaline conditions, the effect of AC surface-coated Cr_2O_3 precipitate on removal performance was not fully understood. This work aimed to study the effect of powdered AC (PAC) surface-formed Cr_2O_3 precipitate on Cr(VI) removal, SEM-EDX (scanning electron microscope-energy dispersive X-ray analysis), and XPS (X-ray photoelectron spectroscopy) were used to investigate the surface morphology and the chemical properties. Desorption and regeneration experiments were used to confirm the role of Cr_2O_3. The insight gained from this study would help to expand the longevity of AC and the recovery of Cr via AC.

2. MATERIALS AND METHODS

2.1. Characterization of PAC particle

To scrutinize the composition of loaded-chromium on PAC after Cr(VI) removal, three types of de-passivation agents were examined to desorb the adsorbed/reduced chromium on PAC. The formation process of the chromium layer on PAC at pH 3 and 7 was inspected by carrying out consecutive desorption tests following each Cr(VI) adsorption. SEM-EDX (JSM-6610LV, JEOL, Japan) and XPS (K-Alpha, Thermo Scientific, USA) were employed to characterize the distribution of chromium and the chemical species of Cr and C on PAC at pH 3 and 7, respectively. The difference of removal mechanisms under the two pH values was delineated by XPS and Raman spectroscopy (DXR, Thermo Scientific, USA).

2.2. Materials

All the chemicals were analytical grade and the aqueous solutions were prepared with deionized water through Barnstead pure II water purification system (Thermo Scientific, USA). Potassium dichromate ($K_2Cr_2O_7$) was purchased from J.T.Baker and used for preparing 1,000 mg/L Cr(VI) as a stock solution. 1.0 M H_2SO_4 and 1.0 M NaOH were used to adjust the pH of the aqueous solutions. H_2SO_4, NaOH, KCl, and 1,5–diphenylcarbazide were provided by J.T.Baker. Commercial available AC was provided by Calgon company, its chemical composition was 97% carbon and 3% inorganic residual. The AC was treated by ball milling and obtained a PAC with an average size of 4 μm, a specific surface area of 929 m^2/g, and a pore radius of 15.9 Å, PAC used in this study was reported in our previous work (Fang *et al.* 2021b). Following the grinding step, the PAC was dried and stored in a desiccator.

2.3. Comparison of Cr(VI) removal at different pH

A comparison was conducted for the PAC removal efficiency at pH 3, 7, and 9 (Jiang *et al.* 2014). The desired mass of PAC (5 g) was mixed with deionized water (100 mL) for 1 h, then the pH was adjusted to 3, 7, and 9 using 1.0 M H_2SO_4 and NaOH aqueous solutions and monitoring the pH with an Orion 3 star pH meter (Thermo Scientific, USA). 0.2829 g $K_2Cr_2O_7$ reagent was added to the PAC suspension to prepare a 1,000 mg/L solution once the pH was stable. To follow the Cr(VI) uptake a 200 μL aliquot was withdrawn from the aqueous solution at 3, 5, 9, 15, 30, 60, 360, and 1,440 min. The withdrawn aliquot was centrifuged in a centrifuge (Allegra™ 21, Beckman Coulter, USA) for 15 min prior to analysis. The Cr(VI) removal capacity was calculated through Equation (1) (Krishna Kumar *et al.* 2019), wherein Γ(mg/g) is the removal capacity, C_0 (mg/L) is the initial concentrations and C_t is the concentration at time t, V (L) and M (g) are the volume of solution and dose of PAC, respectively.

$$\Gamma = (C_0 - C_t)V/M \quad (1)$$

2.4. Selection of desorption agents

Three kinds of desorption agents were evaluated to determine their effectiveness for desorbing the adsorbed chromium species on PAC. Analytical grade $K_2Cr_2O_7$ acted as a precursor of the chromium layer on PAC. To obtain adequate loaded chromium on PAC for assessment, consecutive uptake experiments were undertaken. 5.0 g PAC was mixed with 1,000 mg/L Cr(VI) aqueous solution at a fixed pH of 7 in a glass volumetric flask. This suspension was stirred magnetically (Thermo Scientific, USA) at 100 rpm to prevent deteriorating of the chromium layer formed on the PAC. A 200 μL sample was withdrawn from the suspension at 0.25, 0.5, 1, 3, 5, 7, 9, 12, 15, 30, 60, 120, and 1,440 min to determine the concentration of Cr(VI), then the suspension was filtered to collect the PAC, which was rinsed with deionized water, and dried before the following removal experiments. Consecutive removal steps were performed

with 1,000 mg/L Cr(VI). Dried chromium-loaded PAC after four repetitive adsorption runs was used for the desorption testing. All the batch experiments were conducted in duplicate under ambient conditions. The adsorption capacity at equilibrium for Cr on PAC was expressed as Equation (2)

$$q_p = \sum (1000 - Ce_i)V_i/M_i \quad (2)$$

where q_p (mg/g) is the content of chromium on PAC, Ce_i (mg/L),V_i (mL) and M_i (g) ($i = 1, 2, 3, 4$) are the equilibrium concentration, solution volume and mass of PAC of each removal cycle, respectively.

To desorb the loaded chromium from the PAC, 0.2M KCl, 0.2M H_2SO_4, and 0.1M NaOH were employed. 0.5 g chromium-loaded PAC was mixed with 50 ml of the desorption agent solution in a glass volumetric flask and stirred at 200 rpm, the concentration of desorbed chromium after 1, 3, 5, 7, 9, 24, 30, 48, 72, 96, and 148 h was determined, the efficiency of desorption was determined through Equation (3).

$$\eta = 100 \times (C_t V)/(q_p M) \quad (3)$$

where η (%) is desorption efficiency, C_t (mg/L) is the dissolved chromium concentration at t time, V (L) and M (g) are the volumes of desorption solution and dose of PAC correspondingly. In addition, the performance of PAC treated with Cr(VI) after desorption with different chemical agents was evaluated.

2.5. The formation process of chromium layer at pH 3 and 7

To ascertain the route of the chromium layer formed on PAC, the chromium speciation after consecutive adsorption runs was analyzed with selected desorption agents (0.2M H_2SO_4 and 0.1M NaOH solution). Four desorption tests followed four successive removal cycles were performed and the increment content of loaded chromium on PAC between two successive adsorption runs was determined by Equation (4).

$$\Delta q = (C_{ii} - C_i)V/M \quad (4)$$

where Δq (mg/g) is the increased content of chromium on PAC, C_{ii} and C_i (mg/L) are the equilibrium concentration of desorbed chromium after the two successive elution tests, V (ml) and M (g) are the volume of desorption solution and the dose of PAC after adsorption of Cr(VI).

The adsorption capacity of PAC loaded with chromium on Cr(VI) after the last elution assessment was examined, and all the adsorption experiments were conducted with 1,000 mg/L Cr(VI).

2.6. Analytical method

A colorimetric approach employing 1,5–diphenylcarbazide and a UV-Visible spectrophotometer (Thermo Scientific, USA) coupled with a 1 cm quartz cell was used to determine Cr(VI). 100 μL filtered solution was diluted to 10 ml and mixed with 0.1 mL 49% H_2SO_4, 0.1 mL 42.5% H_3PO_4, and 0.4 mL 0.2% 1,5–diphenylcarbazide solution, sequentially. The mixed solution stood for 10 min and was then measured by a UV-Visible spectrophotometer under 540 nm. The absorbance of deionized water was used as a reference. With prepared 0, 0.02, 0.05, 0.1, 0.2, 0.4, 0.6, 0.8, and 1.0 mg/L Cr(VI), a standard curve of concentration versus absorbance was constructed; this standard curve was used to determine the Cr(VI) concentration of the sample. The total concentration of aqueous Cr was analyzed by atomic absorption spectrometry (AAS, Varian Spectra 220FS), a 50 μL filtered solution was diluted to 10 mL and then sprayed into the flame of air-acetylene. The chromium ground state atoms formed under a high-temperature flame produce selective absorption of the 357.9 nm characteristic spectrum of chromium hollow cathode lamps, and the absorbance value is proportional to the concentration of Cr. The standard curve of total Cr was built in the same way as Cr(VI), and the concentration of total was determined by the standard curve as well. The presence of soluble Cr species in the solution was Cr(III) and Cr(VI), the concentration of aqueous Cr(III) was confirmed by the difference between total Cr and Cr(VI).

3. RESULTS AND DISCUSSION

3.1. Particle characterization

3.1.1. Surface morphology

The surface morphology of PAC after Cr(VI) adsorption under pH 7 was characterized by SEM-EDX and elements mapping. As seen in Figure 1, a chromium layer adsorbed mostly on the PAC surface. A similar observation was reported recently (Wang *et al.* 2020).

3.1.2. XPS spectra analysis

To further inspect the chemical species of Cr on the surface of PAC, XPS analysis was employed. Figure 2(a) and 2(b) show the XPS spectra, which were fitted and deconvoluted into multiple peaks by CasaXPS (version 2.3.23). The peak referenced as C 1 s at 284.8 eV, the Shirley type was designated as the background subtraction. As presented in Figure 2(a), the Cr 2p peak due to Cr(VI), denoted that the Cr(VI) was adsorbed onto PAC. The XPS spectrum of PAC after being treated with Cr(VI) at pH 3 (PAC-pH 3) and 7 (PAC-pH 7) was built as presented in Figure 2(b). The Cr 2p region of the photoelectron spectrum was both detected for PAC-pH 3 and PAC-pH 7, which was consistent with the EDX spectrum shown in Figure 1. Cr 2p involves two energy levels, 2p 1/2 and 2p 3/2. The XPS spectrum of PAC-pH 3 can be divided into the Cr1, Cr2, and Cr3 peaks, where the binding energies (BE) value of Cr1 peak of PAC-pH 3 was 587.5 eV, which was very close to that of Cr_2O_3 (587.4 eV $\pm$ 0.2) (Grohmann *et al.* 1995). The BE for Cr2 and Cr3 of PAC-pH 3 were 579.2 and 577.8 eV, respectively, which can be attributed to Cr(VI) (Murphy *et al.* 2009; Ren *et al.* 2016; Zhang *et al.* 2019). Two contributions of Cr1 and Cr2 for the Cr 2p region of PAC-pH 7 were 587.7 and 578.0 eV, matching well with the binding energy for Cr(VI) and Cr_2O_3 (Biesinger *et al.* 2004; Ren *et al.* 2016; Chen *et al.* 2019). Due to XPS detection depth being no more than 4 nm from the sample surface, it can be said that the chromium layers on the surface of PAC-pH 3 were mainly constituted by Cr(VI) and PAC-pH 7 was mainly constituted by Cr_2O_3(s) (Chowdhury *et al.* 2012). Consistent with the present results, previous studies have demonstrated that the reduction and adsorption participated principally in the Cr(VI) removal on biomass (Wu *et al.* 2010; Cui *et al.* 2011). Moreover, the peak area ratio (Cr1 versus total peaks) as determined by CasaXPS was 69.93% and

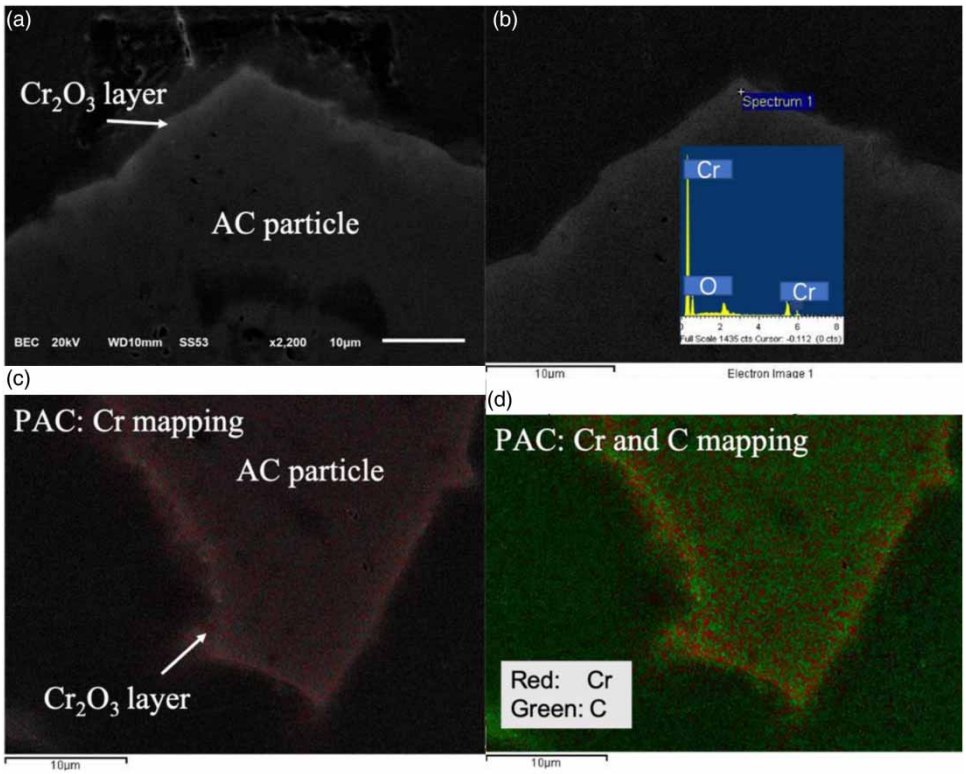

Figure 1 | SEM-EDX micrographs (a and b) and SEM coupling with elements mappings (c and d) of PAC after Cr(VI) adsorption at pH 7.

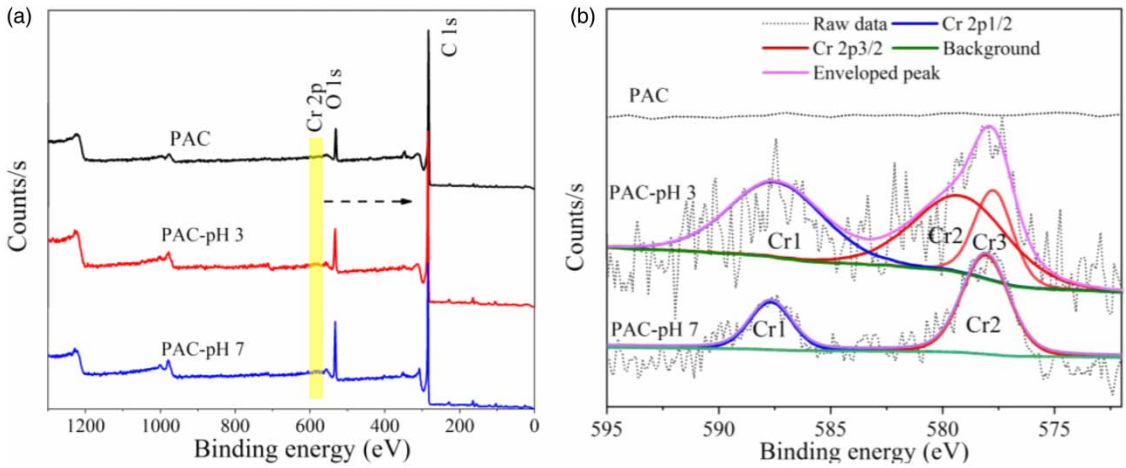

Figure 2 | The XPS spectra of PAC treated with Cr(VI) under pH 3 (PAC-pH 3), pH 7 (PAC-pH 7), and fresh PAC; (a) XPS survey, (b) scan of Cr 2p.

39.91% Cr_2O_3(s) on the surfaces of PAC-pH 7 and PAC-pH 3, respectively. This higher content of Cr_2O_3 on PAC-pH 7 clearly evidenced that more Cr_2O_3 formed on the PAC at pH 7 than at pH 3, impeding the diffusion of Cr(VI) into the PAC, leading to a lower level of Cr(VI) removal. Besides, the ratio of O/C on PAC, PAC-pH 3, and PAC-pH 7 were 0.075, 0.113, and 0.157, respectively (Table 2). This indicates more O on the PAC after adsorption at pH 7 than at pH 3, due to more Cr_2O_3 precipitate. As noted in Table 2, the ratio of Cr/C on PAC-pH 3 was higher than that on PAC-pH 7, which further substantiated that Cr(VI) removal efficiency under pH 3 was superior to that under pH 7 and indicated that not only was there Cr_2O_3 on the PAC surface but also Cr(VI).

The surface functional groups of PAC before and after Cr(VI) adsorption were investigated using high resolution C1 s spectra. The deconvolution of C 1 s produced four peaks, as shown in Figure 3. For PAC, there were four components: C = C (284.8 eV), C-O-C/C-OH (285.5 eV), C-O (286.7 eV), and COOR (286.7 eV) (290.0 eV) (Jieying *et al.* 2014). Similarly, the four peaks of PAC-pH 3 were assigned to the C = C (284.8 eV), C-OH (285.8 eV), C-O (286.5 eV), and COOR (288.7 eV) (Jia & Wang 2015; Ma *et al.* 2018). Meanwhile, the four peaks for PAC-pH 7 were allocated to C = C (284.8 eV), C-OH (285.8 eV), C-O (286.5 eV), and COOR (289.5 eV) (Chen *et al.* 2020). The relative percentages of C-OH for PAC, PAC-pH 3, and PAC-pH 7 were 23.62%, 6.77%, and 6.53%, respectively, which suggested that the group of C-OH contributed to the removal of Cr(VI). The oxidation of C-OH to C-O by Cr(VI) caused the increase of the C-O group (Su *et al.* 2019). Nonetheless, following Cr(VI) adsorption at pH 3, the relative percentage of COOR on PAC rose from 15.22% to 20.56% and dropped to 10.41% after Cr(VI) adsorption at pH 7. This inconsistency may be due to Cr(VI) oxidizing the surface of PAC at pH 3 and introducing more COOR groups (Yin *et al.* 2019), while the Cr(VI) exhibited weak oxidative capacity at higher pH (Gangadharan & Nambi 2014), and the removal of Cr(VI) under pH 7 consumed the COOR groups through the complex.

3.1.3. Raman spectra analysis

Raman spectroscopy investigation was carried out to evaluate the degree of structural order in carbonaceous PACs, as well as to investigate the difference in Cr(VI) removal mechanisms at pH 3 and pH 7. As depicted in Figure 4, the two sharp and strong bands are associated with the D-band (1,319 cm^{-1}. defect with sp^3 bonding) and G-band (1,563 cm^{-1}, graphitization with sp^2 bonding) (Cuesta *et al.* 1994). The intensity ratio of D-band (I_D) versus G-band (I_G) is often used to assess the degree

Table 2 | XPS analysis of PAC before and after treatment with Cr(VI)

Materials	O/C	Cr/C
PAC	0.075	0
PAC-pH 3	0.113	0.005
PAC-pH 7	0.157	0.004

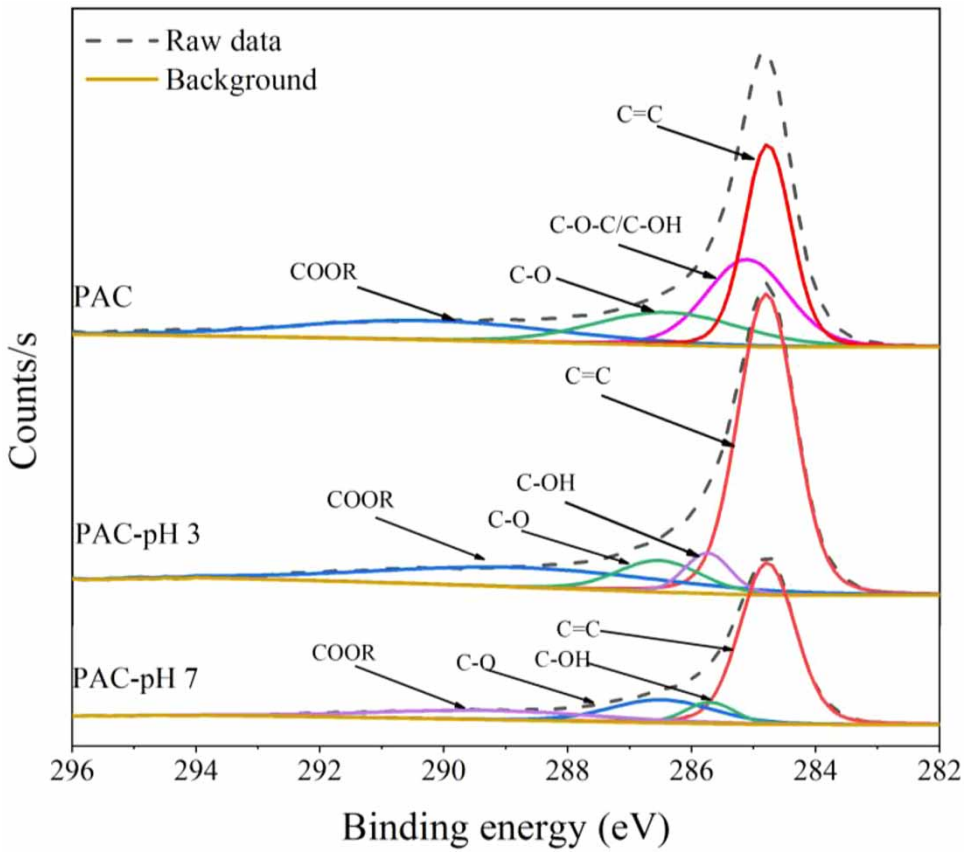

Figure 3 | High resolution C 1 s spectra of PAC, PAC-pH 3, and PAC-pH 7.

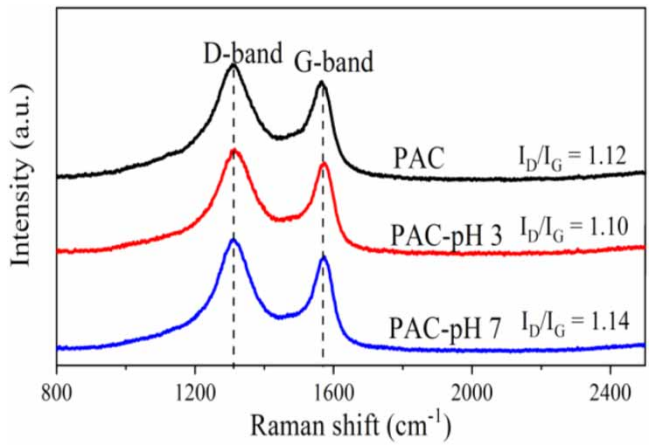

Figure 4 | Raman spectra investigation for pristine PAC, after removal of Cr(VI) at pH 3 and 7.

of disorder in graphite structure in carbon materials (Lespade *et al.* 1984). The value of I_D/I_G declined from 1.12 to 1.10 after treatment at pH 3 but increased from 1.12 to 1.14 after treatment at pH 7. As a result, the existence of defects in PAC was strengthened under pH 7, while at pH 3, a well-organized carbon structure formed. This divergence could be explained by the different Cr(VI) adsorption mechanisms at pH 3 and 7. In general, the reduction of surface oxygen-containing functional groups resulted in the increase of amorphous carbon at pH 7 (Cong *et al.* 2012; Yang *et al.* 2013; Li *et al.* 2016; Wang *et al.* 2017), while the oxidation of hybridized carbon atoms caused structural order to grow at pH 3 (Osswald *et al.* 2006).

3.2. Adsorption performance of PAC at pH 3 and 7

Figure 5 shows a comparison of adsorption performance at pH 3, 7, and 9 for 1,000 mg/L initial concentration of Cr(VI). Adsorption at those three pH values both reached pseudo-equilibrium immediately after 10 mins. Removal capacities for PAC at pH 7 and 3 were 16.8 mg/g and 20 mg/g, respectively, equivalent to 83.86% and nearly 100% removal efficiency. And adsorption capacity under pH 9 was 7.8 mg/g, which was much lower than that at pH 3 and 7. It indicated that the removal performance of PAC on Cr(VI) was higher at low pH, PAC is probably protonated and attracted more anionic Cr(VI).

3.3. Desorption performance of Cr-loaded PAC with chemical agents

The desorption of chromium from the Cr-loaded PAC was evaluated using various chemical agents including H_2SO_4, KCl, and NaOH. Abundant chromium-loaded PAC was prepared at pH 7. As shown in Figure 6, the Cr(VI) elimination experiment using PAC was repeated four times. The duration time for every removal cycle was 24 hours. The next removal cycle began once the previous cycle was completed. After four consecutive repetitive adsorption cycles, the content of chromium on PAC

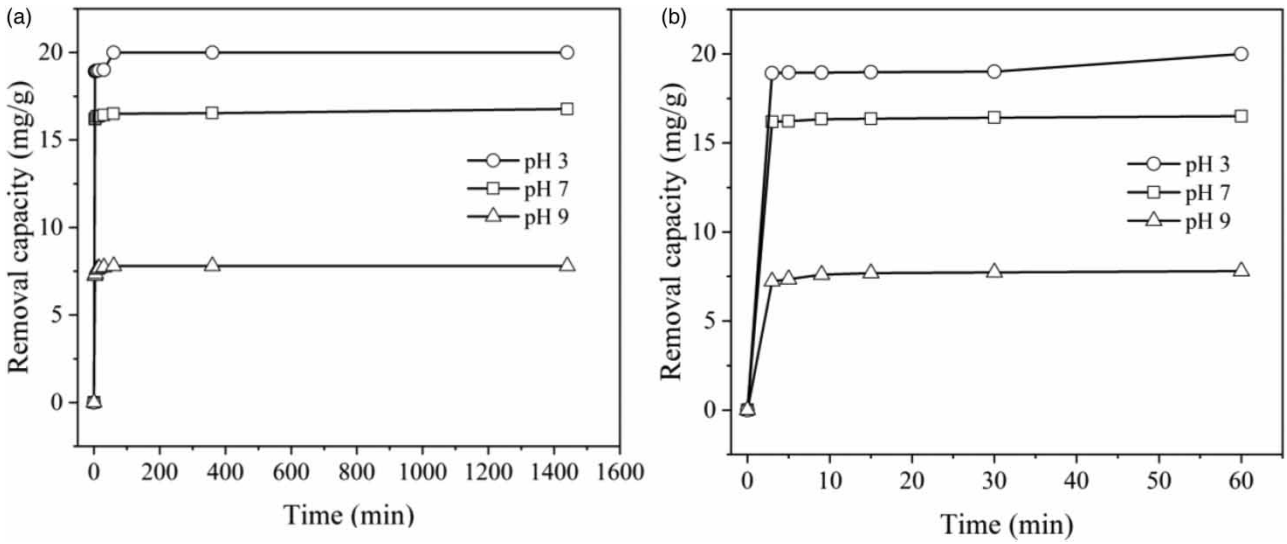

Figure 5 | The adsorption capacities comparison at pH 3, 7, and 9, (a) the full profile of adsorption, (b) the first 60 min adsorption profile (Initial concentration 1,000 mg/L, 50 g/L PAC, 295 K).

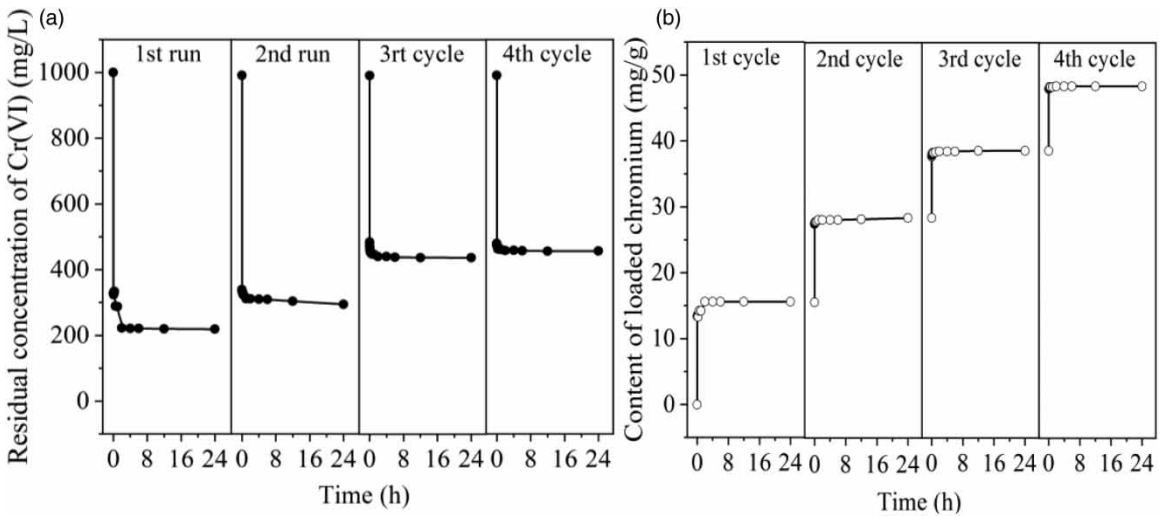

Figure 6 | The preparation of chromium-loaded PAC, (a) the residual concentration of Cr(VI) at each Cr(VI) adsorption cycle, (b) the content of loaded chromium as cycling (1,000 mg/L Cr(VI), 295 K, 50 g/L, pH 7).

reached 48.6 mg/g. The results of the desorption analysis using the three reagents are shown in Figure 7. It is noted that only Cr(III) was dissolved in H_2SO_4 aqueous solutions, whereas Cr(VI) was only desorbed in NaOH aqueous solutions. Negligible Cr(III) or Cr(VI) were detected in the KCl solution when compared to acidic and alkaline aqueous solutions. These findings agree well with Ouki & Neufeld's (1997) findings that 3 g/L Cr(III) and 8.4 g/L Cr(VI) were recovered when exhausted carbon was regenerated under acidic and alkaline conditions, respectively (Ouki & Neufeld 1997). Due to the great stability of the adsorbed chromium on the PAC, desorption of Cr(VI) and Cr(III) from the Cr-loaded PAC with deionized water was minimal. Our results are also in line with those of Jing *et al.* (2011), who found that the desorption rate of Cr-loaded AC was low with distilled water (Jing *et al.* 2011).

As shown in Figure 6(a), Cr(III) precipitate dissolved gradually in 0.2 M H_2SO_4, and 13.0% Cr(III) precipitate was removed under acidic conditions, this process was depicted by Equation (5).

$$Cr_2O_3 + 6H^+ \rightarrow 2Cr^{3+} + 3H_2O \tag{5}$$

With the NaOH aqueous solution (Figure 6(c)), 21.3% Cr(VI) was desorbed, which was higher than the dissolved Cr(III) by the H_2SO_4 aqueous solution. This seems to contradict the XPS conclusion that less Cr(VI) adsorbed on PAC-pH 7 surface. A possible explanation for this might be that more internally adsorbed Cr(VI) in PAC particles was desorbed by alkaline elution. Cr(VI) adsorbed on AC was previously shown to be bound to the surface functional groups (Singha *et al.* 2013). An ion-exchange mechanism could explain the desorption of adsorbed CrO_4^{2-} (the dominant chromium species under alkaline conditions) on surface functional groups by NaOH aqueous solutions, the OH^- ions substituting for CrO_4^{2-} anions, as demonstrated in Equation (6) (Daneshvar *et al.* 2019).

$$PAC - (COOH_2^+)_2 \cdots CrO_4^{2-}(s) + 2OH^- \rightarrow PAC - (COOH)(s) + CrO_4^{2-} + H_2O \tag{6}$$

These findings could be useful in the development of a selective recovery method of Cr(III) and Cr(VI) using acid and alkali aqueous solutions.

3.4. Formation process of chromium layer at pH 3 and 7

To clarify the influence of pH on the development process of the chromium layer on PAC, H_2SO_4, and NaOH desorption agents were used to determine the content of Cr(III) and Cr(VI) adsorbed on PAC-pH 3 and PAC-pH 7. Figure 8 compares

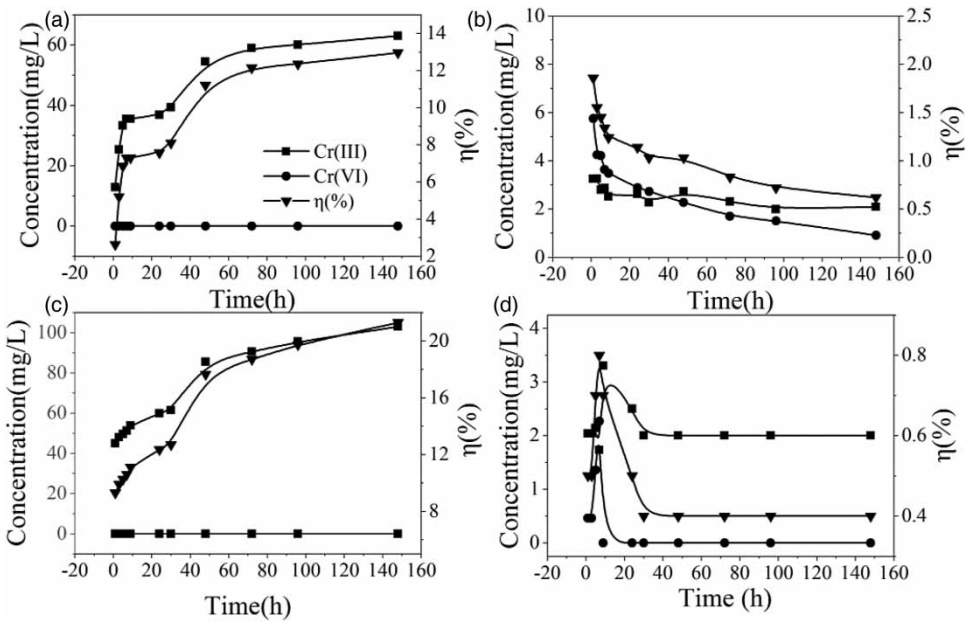

Figure 7 | The effect of chemical agents on desorption performance of Cr-loaded PAC (a) H_2SO_4 (b) KCl (c) NaOH (d) H_2O (0.2M KCl, 0.2M H_2SO_4, 0.1M NaOH, 1 g/100 mL Cr-loaded PAC, 298 K).

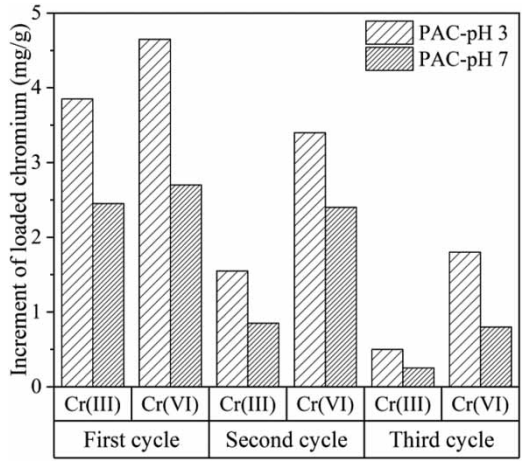

Figure 8 | The increment of chromium loaded on PAC as consecutive Cr(VI) removal cycles (295 K, 50 g/L).

the results obtained from elution tests of PAC-pH 3 and PAC-pH 7 after three consecutive adsorption cycles. It is apparent from the figure that the increment of adsorbed Cr(VI) is higher than reduced Cr(III) at each cycle for both PAC-pH 3 and PAC-pH 7. Hence, it is conceivable to suggest that the adsorption process prevailed for Cr(VI) elimination. This finding was also reported by Daneshvar *et al.* (2019). Another significant observation was that for PAC-pH 3 and PAC-pH 7, the adsorbed Cr(VI) and reduced Cr(III) decreased as the cycles progressed. PAC-pH 3 showed higher Cr(VI) adsorption and reduction capacity. This may be due to the more generated Cr(III) precipitate accumulating on the PAC surface over time at the neutral condition, sheltering the PAC active sites from Cr(VI adsorption.

3.5. Performance of Cr-loaded PAC after desorption

The performance of the PAC for Cr adsorption was assessed after chromium was desorbed from the PAC using the H_2SO_4 and NaOH. Re-adsorption experiments were conducted following the third cycle desorption step. As can be seen in Figure 9, 92.43% removal efficiency of Cr(VI) was achieved by PAC-pH 7 after washing with H_2SO_4, whereas only 51.72% removal was attained using NaOH aqueous. Therefore, it can be inferred that the Cr(III) precipitate is mainly responsible for the poor performance of PAC under neutral conditions. The removal performance after acid washing (92.43%) was higher than the preliminary removal efficiency (83.86%); this result indicated that the acid desorption procedure modified PAC

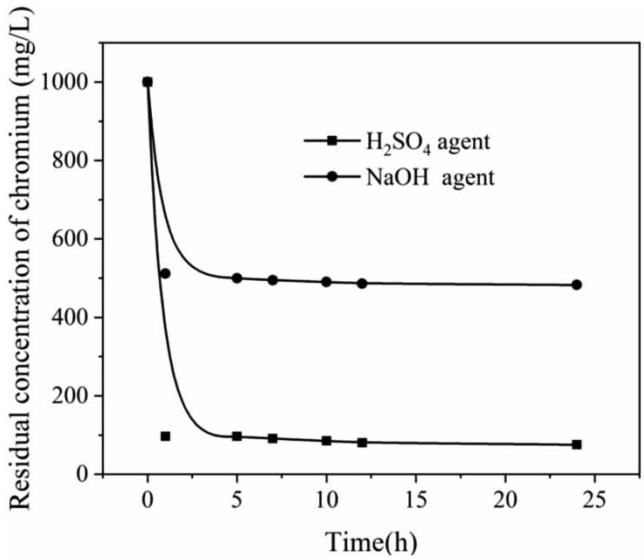

Figure 9 | The activity of chromium-loaded PAC-pH 7 after being treated with H_2SO_4 and NaOH (1,000 mg/L Cr(VI), pH 7).

properties and introduced surface functional groups. These results are consistent with those of Huang *et al.* (2009), who improved AC's Cr(VI) removal capacity by modifying it with nitric acid (Huang *et al.* 2009). As a result, it is proved that PAC's limited removal capability for Cr(VI) at pH 7 was mostly due to Cr(III) precipitate that formed on the surface of PAC. This finding backs the XPS results in that chromium oxide piled up mostly on PAC under neutral conditions. The sulfuric acid proved to be a potential chemical agent for the regeneration of Cr-loaded PAC after treating water contaminated with Cr(VI).

4. CONCLUSIONS

This study aimed to determine the mechanism of the limited sequestration capability of PAC on Cr(VI) under neutral conditions compared to acidic conditions. SEM-EDX substantiated that a chromium layer was formed on PAC, while XPS spectra corroborated the higher Cr_2O_3 content on PAC under alkaline conditions, resulting in poor Cr(VI) removal performance. Conversely, a lower Cr_2O_3 content on PAC under acid conditions is related to the higher Cr(VI) removal capacity. Desorption tests with H_2SO_4 and NaOH solution revealed that the precipitated Cr_2O_3 and adsorbed Cr(VI) can be selectively desorbed, proving that adsorption and reduction processes contributed significantly to the Cr(VI) removal. Consecutive desorption assays proved that the reduction and adsorption capability at 7 declined with time and were both lower than at pH 3. This is due to Cr(III) precipitate and adsorbed Cr(VI) blocking active sites. The superior performance on Cr(VI) removal of Cr-loaded PAC after desorption by H_2SO_4 further confirmed that the restricted removal performance under neutral conditions was ascribed to the formation of a Cr_2O_3 passivation layer on the surface of PAC particles. The insights gained from this work may be of assistance to the recycling of chromium from exhausted AC and extend the lifespan of AC.

ACKNOWLEDGEMENTS

Yi Fang acknowledges CONACYT (National Council of Science and Technology, Mexico) for the Fellowship (No. 900339) to pursue Ph.D. studies in Materials Science and Engineering at the Universidad Autónoma de San Luis Potosí, México. Authors acknowledge the partial financial support by the Guangdong College Students' Innovative Project (pdjh2021b0538, X201910580158), and the Zhaoqing Science and Technology Project (2018N005) to carry out this research.

DATA AVAILABILITY STATEMENT

All relevant data are included in the paper or its Supplementary Information.

REFERENCES

Al-Othman, Z. A., Ali, R. & Naushad, M. 2012 Hexavalent chromium removal from aqueous medium by activated carbon prepared from peanut shell: adsorption kinetics, equilibrium and thermodynamic studies. *Chemical Engineering Journal* **184**, 238–247. https://doi.org/10.1016/j.cej.2012.01.048.

Aparicio, J. D., Lacalle, R. G., Artetxe, U., Urionabarrenetxea, E., Becerril, J. M., Polti, M. A., Garbisu, C. & Soto, M. 2021 Successful remediation of soils with mixed contamination of chromium and lindane: integration of biological and physico-chemical strategies. *Environmental Research* **194**, 110666. https://doi.org/10.1016/j.envres.2020.110666.

Asimakopoulos, G., Baikousi, M., Salmas, C., Bourlinos, A. B., Zboril, R. & Karakassides, M. A. 2021 Advanced Cr(VI) sorption properties of activated carbon produced via pyrolysis of the 'Posidonia oceanica' seagrass. *Journal of Hazardous Materials* **405**, 124274. https://doi.org/10.1016/j.jhazmat.2020.124274.

Barrera-Diaz, C. E., Lugo-Lugo, V. & Bilyeu, B. 2012 A review of chemical, electrochemical and biological methods for aqueous Cr(VI) reduction. *Journal of Hazardous Materials* **223–224**, 1–12. https://doi.org/10.1016/j.jhazmat.2012.04.054.

Biesinger, M. C., Brown, C., Mycroft, J. R., Davidson, R. D. & McIntyre, N. S. 2004 X-ray photoelectron spectroscopy studies of chromium compounds. *Surface and Interface Analysis* **36**, 1550–1563. https://doi.org/10.1002/sia.1983.

Chen, Z., Wei, B., Yang, S., Li, Q., Liu, L., Yu, S., Wen, T., Hu, B., Chen, J. & Wang, X. 2019 Synthesis of PANI/AlOOH composite for Cr(VI) adsorption and reduction from aqueous solutions. *ChemistrySelect* **4**, 2352–2362. https://doi.org/10.1002/slct.201803898.

Chen, X., Wang, X. & Fang, D. 2020 A review on C1s XPS-spectra for some kinds of carbon materials. *Fullerenes, Nanotubes and Carbon Nanostructures* **28**, 1048–1058. https://doi.org/10.1080/1536383X.2020.1794851.

Chowdhury, S. R., Yanful, E. K. & Pratt, A. R. 2012 Chemical states in XPS and Raman analysis during removal of Cr(VI) from contaminated water by mixed maghemite–magnetite nanoparticles. *Journal of Hazardous Materials* 235–236. 246-256, https://doi.org/10.1016/j.jhazmat.2012.07.054.

Cong, H.-P., Ren, X.-C., Wang, P. & Yu, S.-H. 2012 Macroscopic multifunctional graphene-based hydrogels and aerogels by a metal ion induced self-assembly process. *ACS Nano.* **6**, 2693–2703. https://doi.org/10.1021/nn300082 k.

Cruz-Espinoza, A., Ibarra-Galván, V., López-Valdivieso, A. & González-González, J. 2012 Synthesis of microporous eskolaite from Cr(VI) using activated carbon as a reductant and template. *Journal of Colloid and Interface Science* **374**, 321–324. https://doi.org/10.1016/j.jcis.2012.01.059.

Cuesta, A., Dhamelincourt, P., Laureyns, J., Martínez-Alonso, A. & Tascón, J. M. D. 1994 Raman microprobe studies on carbon materials. *Carbon* **32**, 1523–1532. https://doi.org/10.1016/0008-6223(94)90148-1.

Cui, H., Fu, M., Yu, S. & Wang, M. K. 2011 Reduction and removal of Cr(VI) from aqueous solutions using modified byproducts of beer production. *Journal of Hazardous Materials* **186**, 1625–1631. https://doi.org/10.1016/j.jhazmat.2010.12.050.

Daneshvar, E., Zarrinmehr, M. J., Kousha, M., Hashtjin, A. M., Saratale, G. D., Maiti, A., Vithanage, M. & Bhatnagar, A. 2019 Hexavalent chromium removal from water by microalgal-based materials: adsorption, desorption and recovery studies. *Bioresource Technology* **293**, 122064. https://doi.org/10.1016/j.biortech.2019.122064.

Deng, M., Wang, X., Li, Y., Wang, F., Jiang, Z., Liu, Y., Gu, Z., Xia, S. & Zhao, J. 2020 Reduction and immobilization of Cr(VI) in aqueous solutions by blast furnace slag supported sulfidized nanoscale zerovalent iron. *Science of The Total Environment* **743**, 140722. https://doi.org/10.1016/j.scitotenv.2020.140722.

Dognani, G., Hadi, P., Ma, H., Cabrera, F. C., Job, A. E., Agostini, D. L. S. & Hsiao, B. S. 2019 Effective chromium removal from water by polyaniline-coated electrospun adsorbent membrane. *Chemical Engineering Journal* **372**, 341–351. https://doi.org/10.1016/j.cej.2019.04.154.

Duranoğlu, D., Trochimczuk, A. W. & Beker, U. 2012 Kinetics and thermodynamics of hexavalent chromium adsorption onto activated carbon derived from acrylonitrile-divinylbenzene copolymer. *Chemical Engineering Journal* **187**, 193–202. https://doi.org/10.1016/j.cej.2012.01.120.

Fang, Y., Wu, X., Dai, M., Lopez-Valdivieso, A., Raza, S., Ali, I., Peng, C., Li, J. & Naz, I. 2021a The sequestration of aqueous Cr(VI) by zero valent iron-based materials: from synthesis to practical application. *Journal of Cleaner Production* **312**, 127678. https://doi.org/10.1016/j.jclepro.2021.127678.

Fang, Y., Yang, K., Zhang, Y., Peng, C., Robledo-Cabrera, A. & López-Valdivieso, A. 2021b Highly surface activated carbon to remove Cr(VI) from aqueous solution with adsorbent recycling. *Environmental Research* **197**, 111151. https://doi.org/10.1016/j.envres.2021.111151.

Gangadharan, P. & Nambi, I. M. 2014 Hexavalent chromium reduction and energy recovery by using dual-chambered microbial fuel cell. *Water Science and Technology* **71**, 353–358. https://doi.org/10.2166/wst.2014.524.

Grohmann, I., Kemnitz, E., Lippitz, A. & Unger, W. E. S. 1995 Curve fitting of Cr 2p photoelectron spectra of cr2o3 and crf3. *Surface and Interface Analysis* **23**, 887–891. https://doi.org/10.1002/sia.740231306.

Huang, G., Shi, J. X. & Langrish, T. A. G. 2009 Removal of Cr(VI) from aqueous solution using activated carbon modified with nitric acid. *Chemical Engineering Journal* **152**, 434–439. https://doi.org/10.1016/j.cej.2009.05.003.

Ibarra-Galván, V., López-Valdivieso, A., Villavelazquez-Mendoza, C. I., Santoyo-Salazar, J. & Song, S. 2014 Synthesis of eskolaite (α-Cr_2O_3) nanostructures by thermal processing of Cr_2O_3-loaded activated carbon. *Part. Sci. Technol.* **32**, 451–455. https://doi.org/10.1080/02726351.2013.878774.

Jia, Z. & Wang, Y. 2015 Covalently crosslinked graphene oxide membranes by esterification reactions for ions separation. *Journal of Materials Chemistry A* **3**, 4405–4412. https://doi.org/10.1039/C4TA06193D.

Jiang, W., Cai, Q., Xu, W., Yang, M., Cai, Y., Dionysiou, D. D. & O'Shea, K. E. 2014 Cr(VI) adsorption and reduction by humic acid coated on magnetite. *Environmental Science & Technology* **48**, 8078–8085. https://doi.org/10.1021/es405804 m.

Jieying, Z., Zhao, Q. & Ye, Z. 2014 Preparation and characterization of activated carbon fiber (ACF) from cotton woven waste. *Applied Surface Science* **299**, 86–91. https://doi.org/10.1016/j.apsusc.2014.01.190.

Jing, G., Zhou, Z., Song, L. & Dong, M. 2011 Ultrasound enhanced adsorption and desorption of chromium (VI) on activated carbon and polymeric resin. *Desalination.* **279**, 423–427. https://doi.org/10.1016/j.desal.2011.06.001.

Krishna Kumar, A. S., You, J.-G., Tseng, W.-B., Dwivedi, G. D., Rajesh, N., Jiang, S.-J. & Tseng, W.-L. 2019 Magnetically separable nanospherical g-C3N4@Fe_3O_4 as a recyclable material for chromium adsorption and visible-light-driven catalytic reduction of aromatic nitro compounds. *ACS Sustainable Chemistry & Engineering* **7**, 6662–6671. doi:10.1021/acssuschemeng.8b05727.

Lespade, P., Marchand, A., Couzi, M. & Cruege, F. 1984 Caracterisation de materiaux carbones par microspectrometrie Raman. *Carbon* **22**, 375–385. https://doi.org/10.1016/0008-6223(84)90009-5.

Li, Y., Cui, W., Liu, L., Zong, R., Yao, W., Liang, Y. & Zhu, Y. 2016 Removal of Cr(VI) by 3D TiO_2-graphene hydrogel via adsorption enriched with photocatalytic reduction. *Applied Catalysis B: Environmental* **199**, 412–423. https://doi.org/10.1016/j.apcatb.2016.06.053.

Li, J., Zhang, X., Liu, M., Pan, B., Zhang, W., Shi, Z. & Guan, X. 2018 Enhanced reactivity and electron selectivity of sulfidated zerovalent iron toward chromate under aerobic conditions. *Environmental Science and Technology* **52**, 2988–2997. https://doi.org/10.1021/acs.est.7b06502.

Liu, N., Zhang, Y., Xu, C., Liu, P., Lv, J., Liu, Y. & Wang, Q. 2020 Removal mechanisms of aqueous Cr(VI) using apple wood biochar: a spectroscopic study. *Journal of Hazardous Materials* **384**, 121371. https://doi.org/10.1016/j.jhazmat.2019.121371.

Ma, J., Pan, J., Yue, J., Xu, Y. & Bao, J. 2018 High performance of poly(dopamine)-functionalized graphene oxide/poly(vinyl alcohol) nanocomposites. *Applied Surface Science* **427**, 428–436. https://doi.org/10.1016/j.apsusc.2017.07.040.

Ma, H., Yang, J., Gao, X., Liu, Z., Liu, X. & Xu, Z. 2019 Removal of chromium (VI) from water by porous carbon derived from corn straw: influencing factors, regeneration and mechanism. *Journal of Hazardous Materials* **369**, 550–560. https://doi.org/10.1016/j.jhazmat.2019.02.063.

Mohan, D., Singh, K. P. & Singh, V. K. 2005 Removal of hexavalent chromium from aqueous solution using low-cost activated carbons derived from agricultural waste materials and activated carbon fabric cloth. *Industrial and Engineering Chemistry Research* **44**, 1027–1042. https://doi.org/10.1021/ie0400898.

Murphy, V., Tofail, S. A. M., Hughes, H. & McLoughlin, P. 2009 A novel study of hexavalent chromium detoxification by selected seaweed species using SEM-EDX and XPS analysis. *Chemical Engineering Journal* **148**, 425–433. https://doi.org/10.1016/j.cej.2008.09.029.

Niazi, L., Lashanizadegan, A. & Sharififard, H. 2018 Chestnut oak shells activated carbon: preparation, characterization and application for Cr (VI) removal from dilute aqueous solutions. *Journal of Cleaner Production* **185**, 554–561. https://doi.org/10.1016/j.jclepro.2018.03.026.

Norouzi, S., Heidari, M., Alipour, V., Rahmanian, O., Fazlzadeh, M., Mohammadi-moghadam, F., Nourmoradi, H., Goudarzi, B. & Dindarloo, K. 2018 Preparation, characterization and Cr(VI) adsorption evaluation of NaOH-activated carbon produced from date press cake; an agro-industrial waste. *Bioresource Technology* **258**, 48–56. https://doi.org/10.1016/j.biortech.2018.02.106.

Ogata, F., Nagai, N., Itami, R., Nakamura, T. & Kawasaki, N. 2020 Potential of virgin and calcined wheat bran biomass for the removal of chromium(VI) ion from a synthetic aqueous solution. *Journal of Environmental Chemical Engineering* **8**, 103710. https://doi.org/10.1016/j.jece.2020.103710.

Osswald, S., Flahaut, E. & Gogotsi, Y. 2006 In situ Raman spectroscopy study of oxidation of double- and single-wall carbon nanotubes. *Chemistry of Materials* **18**, 1525–1533. https://doi.org/10.1021/cm052755 g.

Ouki, S. K. & Neufeld, R. D. 1997 Use of activated carbon for the recovery of chromium from industrial wastewaters. *Journal of Chemical Technology and Biotechnology* **70**, 3–8. https://doi.org/10.1002/(SICI)1097-4660(199709)70:1<3::AID-JCTB664 > 3.0.CO;2-5.

Qian, L., Liu, S., Zhang, W., Chen, Y., Ouyang, D., Han, L., Yan, J. & Chen, M. 2019 Enhanced reduction and adsorption of hexavalent chromium by palladium and silicon rich biochar supported nanoscale zero-valent iron. *Journal of Colloid and Interface Science* **533**, 428–436. https://doi.org/10.1016/j.jcis.2018.08.075.

Qu, J., Wang, Y., Tian, X., Jiang, Z., Deng, F., Tao, Y., Jiang, Q., Wang, L. & Zhang, Y. 2021 KOH-activated porous biochar with high specific surface area for adsorptive removal of chromium (VI) and naphthalene from water: affecting factors, mechanisms and reusability exploration. *Journal of Hazardous Materials* **401**, 123292. https://doi.org/10.1016/j.jhazmat.2020.123292.

Rakhunde, R., Deshpande, L. & Juneja, H. 2012 Chemical speciation of chromium in water: a review. *Critical Reviews in Environment Science and Technology* **42**, 776–810. https://doi.org/10.1080/10643389.2010.534029.

Ramirez, A., Ocampo, R., Giraldo, S., Padilla, E., Flórez, E. & Acelas, N. 2020 Removal of Cr (VI) from an aqueous solution using an activated carbon obtained from teakwood sawdust: kinetics, equilibrium, and density functional theory calculations. *Journal of Environmental Chemical Engineering* **8**, 103702. https://doi.org/10.1016/j.jece.2020.103702.

Ren, Z., Xu, X., Wang, X., Gao, B., Yue, Q., Song, W., Zhang, L. & Wang, H. 2016 FTIR, Raman, and XPS analysis during phosphate, nitrate and Cr(VI) removal by amine cross-linking biosorbent. *Journal of Colloid and Interface Science* **468**, 313–323. https://doi.org/10.1016/j.jcis.2016.01.079.

Samuel, M. S., Selvarajan, E., Chidambaram, R., Patel, H. & Brindhadevi, K. 2021 Clean approach for chromium removal in aqueous environments and role of nanomaterials in bioremediation: present research and future perspective. *Chemosphere* **284**, 131368. https://doi.org/10.1016/j.chemosphere.2021.131368.

Sangkarak, S., Phetrak, A., Kittipongvises, S., Kitkaew, D., Phihusut, D. & Lohwacharin, J. 2020 Adsorptive performance of activated carbon reused from household drinking water filter for hexavalent chromium-contaminated water. *Journal of Environmental Management* **272**, 111085. https://doi.org/10.1016/j.jenvman.2020.111085.

Shi, Y., Shan, R., Lu, L., Yuan, H., Jiang, H., Zhang, Y. & Chen, Y. 2020 High-efficiency removal of Cr(VI) by modified biochar derived from glue residue. *Journal of Cleaner Production* **254**, 119935. https://doi.org/10.1016/j.jclepro.2019.119935.

Singha, S., Sarkar, U. & Luharuka, P. 2013 Functionalized granular activated carbon and surface complexation with chromates and bi-chromates in wastewater. *Science of the Total Environment* **447**, 472–487. https://doi.org/10.1016/j.scitotenv.2013.01.006.

Su, M., Fang, Y., Li, B., Yin, W., Gu, J., Liang, H., Li, P. & Wu, J. 2019 Enhanced hexavalent chromium removal by activated carbon modified with micro-sized goethite using a facile impregnation method. *Sci Total Environ.* **647**, 47–56. https://doi.org/10.1016/j.scitotenv.2018.07.372.

Valentín-Reyes, J., García-Reyes, R., García-González, A., Soto-Regalado, E. & Cerino-Córdova, F. 2019 Adsorption mechanisms of hexavalent chromium from aqueous solutions on modified activated carbons. *Journal of Environmental Management* **236**, 815–822. https://doi.org/10.1016/j.jenvman.2019.02.014.

Wang, X., Liang, Y., An, W., Hu, J., Zhu, Y. & Cui, W. 2017 Removal of chromium (VI) by a self-regenerating and metal free g-c3n4/graphene hydrogel system via the synergy of adsorption and photo-catalysis under visible light. *Applied Catalysis B: Environmental* **219**, 53–62. https://doi.org/10.1016/j.apcatb.2017.07.008.

Wang, C., Wu, Y., Qu, T., Liu, S., Pi, Y. & Shen, J. 2019 Enhanced Cr (VI) removal in the synergy between the hydroxyl-functionalized ball-milled ZVI/Fe3O4 composite and Na2EDTA complexation. *Chemical Engineering Journal* **359**, 874–881. https://doi.org/10.1016/j.cej.2018.11.104.

Wang, Y., Peng, C., Padilla-Ortega, E., Robledo-Cabrera, A. & López-Valdivieso, A. 2020 Cr(VI) adsorption on activated carbon: mechanisms, modeling and limitations in water treatment. *Journal of Environmental Chemical Engineering* **8**, 104031. https://doi.org/10.1016/j.jece.2020.104031.

Wu, J., Zhang, H., He, P.-J., Yao, Q. & Shao, L.-M. 2010 Cr(VI) removal from aqueous solution by dried activated sludge biomass. *Journal of Hazardous Materials* **176**, 697–703. https://doi.org/10.1016/j.jhazmat.2009.11.088.

Wu, M., Li, Y., Li, J., Wang, Y., Xu, H. & Zhao, Y. 2019 Bioreduction of hexavalent chromium using a novel strain CRB-7 immobilized on multiple materials. *Journal of Hazardous Materials* **368**, 412–420.

Wu, F., Zhao, T., Yao, Y., Jiang, T., Wang, B. & Wang, M. 2020 Recycling supercapacitor activated carbons for adsorption of silver (I) and chromium (VI) ions from aqueous solutions. *Chemosphere* **238**, 124638. https://doi.org/10.1016/j.chemosphere.2019.124638.

Yang, X., Cui, H., Li, Y., Qin, J., Zhang, R. & Tang, H. 2013 Fabrication of Ag_3PO_4-Graphene composites with highly efficient and stable visible light photocatalytic performance. *ACS Catalysis* **3**, 363–369. 10.1021/cs3008126.

Yin, W., Guo, Z., Zhao, C. & Xu, J. 2019 Removal of Cr(VI) from aqueous media by biochar derived from mixture biomass precursors of *Acorus calamus* Linn. and feather waste. *Journal of Analytical and Applied Pyrolysis* **140**, 86–92. https://doi.org/10.1016/j.jaap.2019.04.024.

Zeng, Q., Hu, Y., Yang, Y., Hu, L., Zhong, H. & He, Z. 2019 Cell envelope is the key site for Cr (VI) reduction by *Oceanobacillus oncorhynchi* W4, a newly isolated Cr (VI) reducing bacterium. *Journal of Hazardous Materials* **368**, 149–155. https://doi.org/10.1016/j.jhazmat.2019.01.031.

Zhang, Y.-J., Ou, J.-L., Duan, Z.-K., Xing, Z.-J. & Wang, Y. 2015 Adsorption of Cr(VI) on bamboo bark-based activated carbon in the absence and presence of humic acid. *Colloids and Surfaces A: Physicochemical and Engineering Aspects* **481**, 108–116. https://doi.org/10.1016/j.colsurfa.2015.04.050.

Zhang, L., Fu, F. & Tang, B. 2019 Adsorption and redox conversion behaviors of Cr(VI) on goethite/carbon microspheres and akaganeite/carbon microspheres composites. *Chemical Engineering Journal* **356**, 151–160. https://doi.org/10.1016/j.cej.2018.08.224.

Zhang, L., Qiu, Y.-Y., Zhou, Y., Chen, G.-H., van Loosdrecht, M. C. M. & Jiang, F. 2021a Elemental sulfur as electron donor and/or acceptor: mechanisms, applications and perspectives for biological water and wastewater treatment. *Water Research* **202**, 117373. https://doi.org/10.1016/j.watres.2021.117373.

Zhang, W., Qian, L., Chen, Y., Ouyang, D., Han, L., Shang, X., Li, J., Gu, M. & Chen, M. 2021b Nanoscale zero-valent iron supported by attapulgite produced at different acid modification: synthesis mechanism and the role of silicon on Cr(VI) removal. *Chemosphere* **267**, 129183. https://doi.org/10.1016/j.chemosphere.2020.129183.

Zhou, L., Liu, Y., Liu, S., Yin, Y., Zeng, G., Tan, X., Hu, X., Hu, X., Jiang, L., Ding, Y., Liu, S. & Huang, X. 2016 Investigation of the adsorption-reduction mechanisms of hexavalent chromium by ramie biochars of different pyrolytic temperatures. *Bioresource Technology* **218**, 351–359. https://doi.org/10.1016/j.biortech.2016.06.102.

First received 11 August 2021; accepted in revised form 29 September 2021. Available online 12 October 2021